Universal Spectrum of Two-Dimensional Turbulence on a Rotating Sphere and Some Basic Features of Atmospheric Circulation on Giant Planets

Semion Sukoriansky*

Department of Mechanical Engineering/Perlstone Center for Aeronautical Engineering Studies, Ben-Gurion University of the Negev, Beer-Sheva, Israel

Boris Galperin

College of Marine Science, University of South Florida, St. Petersburg, Florida 33701

Nadejda Dikovskaya

Department of Mechanical Engineering, Ben-Gurion University of the Negev, Beer-Sheva, Israel

(Received 14 March 2002; published 28 August 2002)

The Kolmogorov-Batchelor-Kraichnan (KBK) theory of two-dimensional turbulence is generalized for turbulence on the surface of a rotating sphere. The energy spectrum develops considerable anisotropy; a steep -5 slope emerges in the zonal direction, while in all others the classical KBK scaling prevails. This flow regime in robust steady state is reproduced in simulations with linear drag. The conditions favorable for this regime may be common for giant planets' atmospheric circulations; the same steep spectra are found in their observed zonal velocity profiles and utilized to explain their basic characteristics.

DOI: 10.1103/PhysRevLett.89.124501 PACS numbers: 47.27.Eq, 47.32.–y, 96.30.–t

Two-dimensional rotating turbulent flows with nonzero gradient of ambient vorticity, such as flows on the surface of a rotating sphere, are important for understanding large-scale terrestrial and planetary circulations. Such flows exhibit anisotropic behavior highlighted by energetic alternating zonal jets. This behavior is a manifestation of a hydrodynamic regime with a highly anisotropic spectrum. In this Letter, we generalize the Kolmogorov-Batchelor-Kraichnan (KBK) theory to include the new regime and demonstrate its realizability in steady state. Some of the problematics of that regime are similar to those of forced nonrotating 2D turbulence, and we start with a brief survey of the latter case. Forced, isotropic 2D turbulence is described by the KBK theory that is based upon two invariants, ϵ and η, the rates of spectral transfers of energy and enstrophy. Simultaneous energy and enstrophy cascades cannot coexist in the same spectral range giving rise to the downscale (direct) enstrophy and upscale (inverse) energy cascades. The inverse cascade renders 2D turbulence nondissipative and unsteady. In an unbounded domain, one can define a quasisteady state in which the modes swept by the inverse cascade remain in steady state and comprise the energy range. In that range, the one-dimensional spectral energy density E (energy per mode n; n being the total wave number in the spherical harmonics expansion) depends on ϵ and n only, leading to celebrated KBK spectrum

$$E(n) = C_K \epsilon^{2/3} n^{-5/3}, \tag{1}$$

C_K being the Kolmogorov-Kraichnan constant whose accepted value is $C_K \simeq 6$ in both planar and spherical [1] geometries. The inverse cascade and ensuing large-scale energy condensation [2] render steady-state simulations in a bounded domain unfeasible without some kind of a large-scale energy withdrawal mechanism. If such a mechanism (drag) is introduced, its effect is assumed to be confined to the range $n < n_{fr}$, n_{fr} being the frictional wave number. The modes $n > n_{fr}$ comprise the inertial range with the energy spectrum (1). Flows of this kind were indeed produced both experimentally [3,4] and computationally [5,6]. The existence of KBK inertial range critically depends on drag's representation. Various high-power inverse Laplacian (hypofriction) formulations have been employed to ensure sharp energy cutoff for $n < n_{fr}$ and enlarge the inertial range. However, in long integrations, even if initial spectrum adheres to (1), energy tends to accumulate in the lowest modes leading to spectral steepening and eventual disappearance of the KBK scaling [7,8]. Such behavior can be traced to the distortion of the inverse cascade due to abrupt falloff of the spectrum at $n < n_{fr}$. Triad interactions that include quashed modes become inactive and facilitate energy accumulation in unquashed modes. This problem can be alleviated with the use of a two-parametric large-scale drag representation designed to emulate undistorted energy transfer by triad interactions [6]. This representation is close to the linear drag. Most experimental and numerical investigations in which the robust steady-state KBK regime was obtained employed linear drag. Mimicking soft damping processes such as friction in Ekman boundary layers [9], linear drag is quite common in nature. The high-power hypofriction parametrizations, on the other hand, do not represent any known physical processes, and their utility for simulation of realistic flows is questionable.

When rotation is present, 2D turbulence preserves two invariants and inverse cascade that hampers attaining the steady state. The analysis of quasisteady state should now include two new parameters, Ω/R and m, Ω and R being the angular velocity and the radius of the sphere, respectively, and m being the zonal wave number. These parameters appear in Navier-Stokes and vorticity equations and form two additional independent dimensionless groups. The generalized nondimensional expression for E becomes anisotropic,

$$\Pi_1 = f(\Pi_2, \Pi_3), \tag{2}$$

where $\Pi_1 = E/[(\Omega/R)^2 n^{-5}]$, $\Pi_2 = n/n_\beta$, $\Pi_3 = m/n$, and $n_\beta = [(\Omega/R)^3/\epsilon]^{1/5}$. The analytical representation of the function f can be determined from quasisteady state simulations [1,10,11]. For $\Pi_2 < 1$ and $\Pi_3 \to 0$, f approaches a constant value of $C_Z = O(1)$. In the opposite limit $\Pi_2 \to \infty$, the flow becomes isotropic and f is independent of Π_3 and Ω/R; then, the dependence $f \propto (n/n_\beta)^{10/3}$ recovers the KBK scaling. The same scaling extends for $\Pi_2 < 1$ and $\Pi_3 \neq 0$. Synthesizing all information, obtain the anisotropic spectral scaling of 2D turbulence on rotating sphere in quasisteady state,

$$E(n, m/n) = C_K \epsilon^{2/3} n^{-5/3}, \qquad m/n \neq 0, \tag{3}$$

$$E(n, m/n) = C_Z (\Omega/R)^2 n^{-5}, \qquad m/n \to 0, \quad n/n_\beta < 1. \tag{4}$$

Numerical simulations on both the β-plane [10] and rotating sphere [1] give $C_Z \simeq 0.5$.

The k^{-5} spectrum on the β-plane was discussed by Rhines [12] based upon dimensional considerations. Rhines noted that such a steep spectrum must be nonlocal and depend on low modes, thus negating the initial scaling; spectral anisotropy was excluded in this analysis. For some time, this controversy has hampered further exploration of the spectrum. The present results demonstrate that this steep spectrum is a component of the anisotropic spectrum (3) and (4). The impact of the ambient vorticity gradient on 2D turbulence is threefold: the energy flux becomes reorientated into zonal flow [10]; the stability of the zonal flow is enhanced, via Rayleigh-Kuo criterion [10]; the spectrum (4) imposes an upper limit on the energetic capacity of zonal modes and thus represents a saturation spectrum [1].

A fundamental question is the reproducibility of the new regime in robust steady state, i.e., in flows with small-scale forcing and large-scale drag.

To address this issue, a series of long-term simulations with a linear drag were performed using a barotropic 2D vorticity equation on the surface of a rotating sphere with the radius $R = 1$. A Gaussian grid was employed with 400×200 resolution (400 nodes in longitude, 200 nodes in latitude) and 2/3 dealiasing rule (R133 rhomboidal truncation). Simulations differed in both Ω and ϵ. The Gaussian random forcing was distributed among all modes $n = 83, 84, 85$ with constant variance; it was uncorrelated in time and between the modes.

The energy spectra in spherical geometry were calculated as $E(n) = \frac{n(n+1)}{4R^2} \sum_{m=-n}^{n} \langle |\psi_n^m|^2 \rangle$, where ψ_n^m is the coefficient with the spherical harmonic Y_n^m in stream function decomposition, and the brackets indicate an ensemble or time average [13,14]. Introduce zonal and residual spectra according to $E(n) = E_Z(n) + E_R(n)$, where the former corresponds to the addend with $m = 0$; E_Z and E_R intersect at $n_i = (C_Z/C_K)^{3/10} n_\beta$. Introduce also a zonal spectrum per mode m and n, $E_Z^0(n) = E_Z(n)/\Delta m$, where $\Delta m = 1$. Numerically, this spectrum is congruent to (4). For large n, when the spectrum is nearly isotropic, $E_Z^0(n) = C_K \epsilon^{2/3} n^{-5/3}/(2n+1) \simeq (1/2) C_K \epsilon^{2/3} n^{-8/3}$. For that spectrum, the transition between -5 and $-8/3$ scaling exponents takes place at $n_z = (2C_Z/C_K)^{3/7} (n_\beta/\Delta m)^{3/7} n_\beta$.

We report results of three simulations; their respective parameters are summarized in Table I. The natural time scale was $\tau = \Omega^{-1}$. In all simulations, executed for the total time in excess of 100 000 days, a robust steady state had been attained after about 10 000 days. The flow field exhibited slow variability such that proper spectral estimates required long and tedious averaging. Figure 1(a) shows a typical sample of the instantaneous zonal spectrum. Although it appears to follow the scaling (4) in general, it exhibits large fluctuations exceeding at times 2 orders of magnitude. The corresponding average spectra were calculated using about 2000 samples separated by time intervals of 40 days; they are shown in Figs. 1(b)–1(d). In all three simulations, the averaged spectra appear smooth; the zonal spectra are in good agreement with Eq. (4), and the residual spectra agree well with the Kolmogorov spectrum (3). The transition from the $-8/3$ to -5 slope takes place around n_z which is apparent in Figs. 1(c) and 1(d). At $n < n_i$, a single zonal mode holds more energy than all the nonzonal modes together. At about n_{fr}, the spectra appear to start leveling off. The zonal energy "spills" into adjacent modes at low n. Finally, it is emphasized that the zonal spectra in steady state are independent of ϵ. In summary, these simulations confirm the existence of the new flow regime in steady state and demonstrate its peculiar connection with the isotropic KBK scaling in the spectral region where flow is strongly anisotropic and dominated by Rossby waves.

The new flow regime has not yet been produced experimentally. However, the upper atmospheres of four

TABLE I. Parameters of simulations on rotating sphere.

Simulation	ϵ	Ω	n_{fr}	n_β	n_i	n_z
S1	ϵ_0	Ω_0	7.7	38.3	18.2	84.8
S2	ϵ_0	$0.5\Omega_0$	5.5	25.2	12	46.6
S3	$5\epsilon_0$	Ω_0	7.7	27.7	13.1	53.4

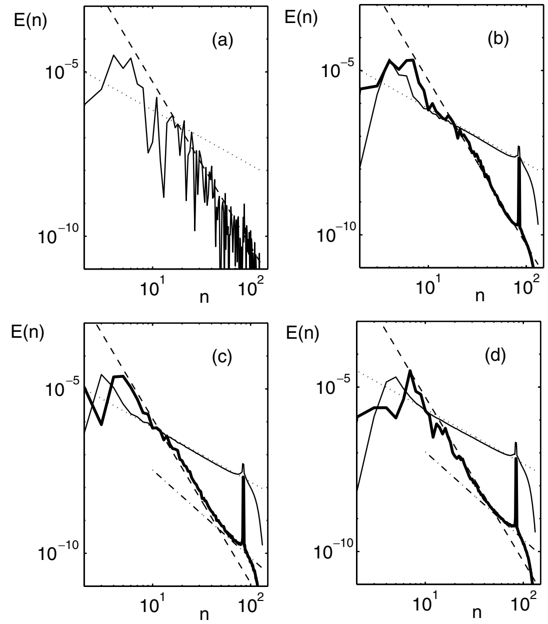

FIG. 1. Instantaneous zonal spectrum (a) and averaged zonal (thick lines) and residual (thin lines) spectra in simulations S1–S3 [(b)–(d), respectively] of 2D turbulence on rotating sphere. Dashed, dotted, and dash-dotted lines represent $0.5(\Omega/R)^2 n^{-5}$, $6\epsilon^{2/3}n^{-5/3}$, and $3\epsilon^{2/3}n^{-8/3}$ spectra, respectively.

giant planets of our solar system, gas giants Jupiter and Saturn and ice giants Uranus and Neptune, present gigantic natural laboratories where this regime can materialize. Because of the absence of solid surfaces and adjacent boundary layers, the giant planets' atmospheres are characterized by relatively weak friction (low n_{fr}). Fast rotation and relatively weak forcing, particularly on the ice giants, result in large n_β. The effect of the vertical density stratification is important on scales smaller than the Rossby deformation radius [9]. On the giant planets, these scales are smaller than n_β^{-1}. Scales beyond the Rossby radius are characterized by barotropic dynamics [15,16]. There are indications that 3D barotropic flows with strong rotation and small aspect ratio undergo "two-dimensionalization" and develop flow regime with the $-5/3$ spectrum in the horizontal [11]. Such flows may undergo further "one-dimensionalization" in the spectral range $n \in (n_{fr}, n_\beta)$, giving rise to a regime with the zonal spectrum (4). Indeed, the spectra of the large-scale zonal circulations on the gas giants agree with (4) both in the slope and in the magnitude [17]. Here the analysis is extended to incorporate new data for Jupiter and to include the ice giants whose characteristics are significantly different from those of the gas giants. The results are shown in Fig. 2. The observed profiles of the large-scale atmospheric circulations are, in fact, single realizations of turbulent flow fields; large fluctuations, at times exceeding 2 orders of magnitude, resemble those detected in simulations, Fig. 1(a). In the range $n < n_{fr}$, the spectra tend to level off, consistently with the action of some kind of a large-scale drag. The rapid drops in the spectra in the vicinity of n_{fr} are similar to that in simulated instantaneous spectrum, Fig. 1(a). For the ice giants, the data are scarce and insufficient for meaningful spectral analysis; instead, we have used analytical expressions interpolating the data [20,21]. In the inertial range $n > n_{fr}$, the spectra on Jupiter, Saturn, and Neptune are in good agreement with the theoretical spectrum (4) with regard to both the slope and the magnitude. For Uranus, the data are extremely scarce, but even in this case, the mode $n = 3$ appears to belong on the theoretical line. Observe that the agreement of the zonal spectra with (4) on all four planets confirms its independence of ϵ; the total kinetic energy is determined by Ω, R, and n_{fr} only. Using a simple conceptual model that assumes a constant spectrum for $n < n_{fr}$ and (4) for $n > n_{fr}$, and integrating from 0 to ∞, an equation for the total kinetic energy of atmospheric circulation on giant planets can be derived,

$$E_{\mathrm{tot}} = \tfrac{5}{4}C_Z(\Omega/R)^2 n_{fr}^{-4}. \tag{5}$$

Defining an averaged velocity as $U = (2E_{\mathrm{tot}})^{1/2}$, find $n_{fr} \approx n_R$, where $n_R = [(\Omega/R)/U]^{1/2}$ is the Rhines's wave number. Note that the modes around n_R contain most of the energy and their signature dominates the zonal velocity profile. Thus, Rn_R is roughly equal to the number of zonal jets. A scale equivalent to n_R^{-1} was introduced by Hide [22] to characterize the widths of the equatorial flows on Jupiter and Saturn. Although the precise physics of the large-scale friction on giant planets is still unknown, it is reasonable to assume that the friction is ultimately related to 3D turbulence and that higher values of forcing ϵ would be accompanied by higher turbulence intensity and a higher rate of dissipation or, equivalently, higher values of n_{fr}. Assume that ϵ is some fraction of the energy obtained from the solar heating (internal energy sources may roughly double its value [23]) and is thus decreasing with increasing distance away from the Sun such that n_{fr} also decreases in the order from Jupiter to Neptune. Indeed, using the *observed* values of E_{tot}, find $n_R \simeq n_{fr} \simeq 13$, 6.9, 3.9, and 2.6 for Jupiter, Saturn, Uranus, and Neptune, respectively. This observation, combined with the dependence of E_{tot} on Ω, R, and n_{fr} and independence of ϵ is critical for understanding the energetics of atmospheric circulations on giant planets. It also resolves the mystery of circulation on Saturn being stronger than that on Jupiter and circulation on Neptune being stronger than that on Uranus, although the former planets are farther away from the Sun and are expected to have weaker forcing. Applied to the ice giants, same ideas suggest that even though the forcing there is minuscule, acting over a very long time, it is nevertheless sufficient to spin up circulations with considerable kinetic energies; in fact, Neptune, that is, the giant planet farthest away from the Sun, has the most energetic circulation in the solar system. These

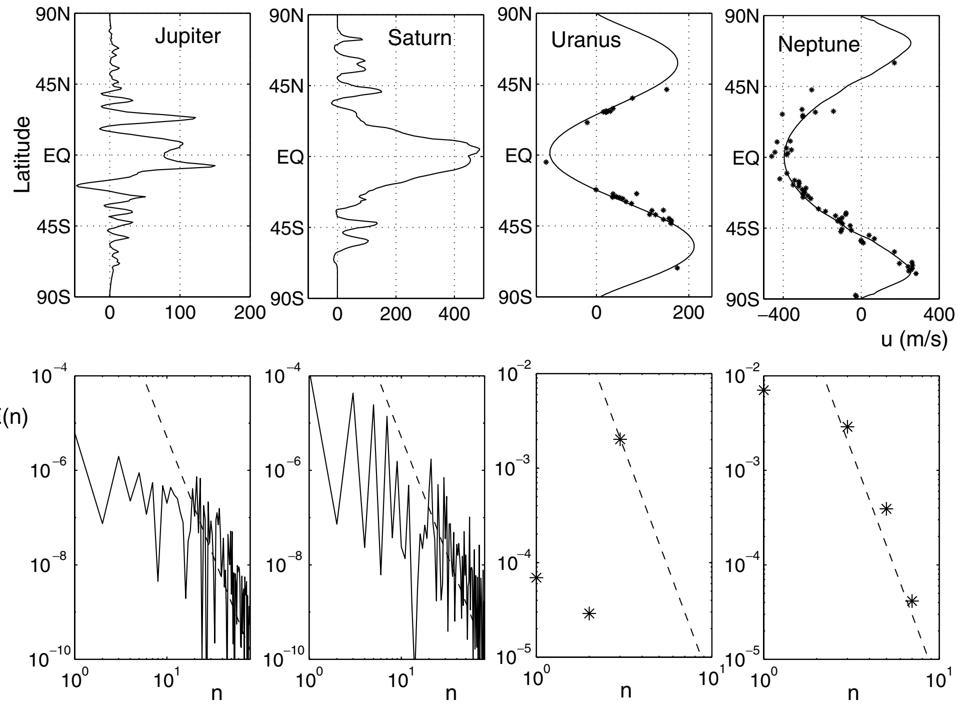

FIG. 2. Top row: observed zonal profiles deduced from the motion of the cloud layers [18–21]; bottom row: observed zonal spectra (solid lines and asterisks) and theoretical zonal spectra Eq. (4) (dashed lines) on the giant planets [all spectra are normalized with their respective values of $(\Omega/R)^2$].

results may also be instrumental for quantifying basic parameters of circulation on extrasolar giant planets when proper data become available.

In summary, rotating 2D flows with nonzero gradient of ambient vorticity, under some circumstances, develop a fundamentally new, anisotropic flow regime where most of the energy resides in zonal jets, while its level is independent of forcing. Spectra of these flows, given by Eqs. (3) and (4) with universal constant $C_Z \simeq 0.5$, can be derived by combining computer simulations and extended KBK-type dimensional analysis. Systems favoring this regime are characterized by low friction and fast rotation; among naturally occurring environments that can harbor this regime are the atmospheres of giant planets.

The authors are thankful to Joseph Tribbia of NCAR who kindly provided the code solving the barotropic vorticity equation on a sphere, Julian Hunt for pointing our attention to the paper by Hide and for several illuminating discussions, and CARTUM scientists for their keen interest and encouragement. Support by the ARO Grant No. DAAD19-01-1-0816 is gratefully acknowledged.

*Electronic address: semion@bgumail.bgu.ac.il

[1] H.-P. Huang, B. Galperin, and S. Sukoriansky, Phys. Fluids **13**, 225 (2001).
[2] L. Smith and V. Yakhot, Phys. Rev. Lett. **71**, 352 (1993).
[3] J. Sommeria, J. Fluid Mech. **170**, 139 (1986).
[4] J. Paret and P. Tabeling, Phys. Rev. Lett. **79**, 4162 (1997).
[5] M. Maltrud and G. Vallis, J. Fluid Mech. **228**, 321 (1991).
[6] S. Sukoriansky, B. Galperin, and A. Chekhlov, Phys. Fluids **11**, 3043 (1999).
[7] V. Borue, Phys. Rev. Lett. **72**, 1475 (1994).
[8] S. Danilov and D. Gurarie, Usp. Fiz. Nauk **170**, 921 (2000) [Sov. Phys. Usp. **43**, 863 (2000)].
[9] J. Pedlosky, *Geophysical Fluid Dynamics* (Springer-Verlag, Berlin, 1987), 2nd ed.
[10] A. Chekhlov, S. Orszag, S. Sukoriansky, B. Galperin, and I. Staroselsky, Physica (Amsterdam) **98D**, 321 (1996).
[11] L. Smith and F. Waleffe, Phys. Fluids **11**, 1608 (1999).
[12] P. Rhines, J. Fluid Mech. **69**, 417 (1975).
[13] G. Boer, J. Atmos. Sci. **40**, 154 (1983).
[14] G. Boer and T. Shepherd, J. Atmos. Sci. **40**, 164 (1983).
[15] P. Rhines, Annu. Rev. Fluid Mech. **11**, 401 (1979).
[16] R. Panetta, J. Atmos. Sci. **50**, 2073 (1993).
[17] B. Galperin, S. Sukoriansky, and H.-P. Huang, Phys. Fluids **13**, 1545 (2001).
[18] E. Garcýa-Melendo and A. Sanchez-Lavega, Icarus **152**, 316 (2001).
[19] A. Sanchez-Lavega, J. Rojas, and P. Sada, Icarus **147**, 405 (2000).
[20] H. Hammel, K. Rages, G. Lockwood, E. Karkoschka, and I. de Pater, Icarus **153**, 229 (2001).
[21] L. Sromovsky, P. Fry, T. Dowling, K. Baines, and S. Limaye, Icarus **149**, 459 (2001).
[22] R. Hide, Planet. Space Sci. **14**, 669 (1966).
[23] I. de Pater and J. Lissauer, *Planetary Sciences* (Cambridge University Press, Cambridge, U.K., 2001).